

Thermal conductivity calculation of magnetite using molecular dynamics simulation

Authors

Masoud Jedari Ghourichaei ^a
Mohammad Goharkhah ^{a*}
Naiyer Razmara ^b

^a Faculty of Mechanical Engineering, Sahand University of Technology, Tabriz, Iran

^b Department of Mechanical Engineering, Azarbaijan Shahid Madani University, Tabriz, Iran

Article history:

Received : 19 April 2019

Accepted : 3 November 2019

Keywords: Molecular Dynamics, Thermal Conductivity, Magnetite, rNEMD.

ABSTRACT

In the current research, thermal conductivity of magnetite (Fe_3O_4) has been calculated using molecular dynamic simulation. The rNEMD Molecular Dynamics Method provided in the LMMPS package is used for the simulation of the thermal conductivity. The effects of magnetite layer size and temperature on the thermal conductivity have been investigated. The numerical results have been validated by experimental data. Results show that the thermal conductivity of magnetite can be predicted appropriately using Buckingham potential function. Moreover, Thermal conductivity of magnetite is shown to be a decreasing function of temperature. The obtained results provide a benchmark for magnetite ferrofluid heat transfer simulations, which has been extensively increased in recent years.

1. Introduction

Magnetite nanofluid is a colloidal mixture of magnetite nanoparticles, which is suspended in a carrier fluid (typically water or oil). Recently, this nanofluid has received extensive attention from the researchers due to its application as a coolant in micro heat exchangers, microgravity conditions, MEMS devices, and electronic cooling [1-2]. The design and thermal management of such systems require reliable thermal conductivity data of magnetite. Several methods such as transient hot wire and three-omega ($3-\omega$) have been used previously for thermal conductivity measurement of magnetite. Molgard and Smeltzer [3] measured

the thermal conductivity of magnetite and hematite experimentally over the temperature range of 340K-675K. They observed that the thermal conductivity decreases with temperature. Clark [4] carried out an experimental study and reported a value of 5.2 W/m.K for the thermal conductivity of bulk magnetite at the temperature of 293K. Furthermore, Park et al. [5] obtained the thermal conductivity of epitaxial Fe_3O_4 thin films using a four-point probe $3-\omega$ method. The thicknesses of the thin films were between 100 and 400 nm and were prepared on SiO_2/Si substrates. They revealed that the thermal conductivities of the thin films are significantly reduced compared with those of the corresponding bulk materials.

Previous experimental results indicate that the thermal conductivity of magnetite has a decreasing trend with temperature. Moreover, the thickness of the magnetite is shown to have a significant effect on thermal conductivity.

* Corresponding author: Mohammad Goharkhah
Faculty of Mechanical Engineering, Sahand University of Technology, Tabriz, Iran
Email: goharkhah@sut.ac.ir

That is, the measured values generally fluctuate by changing the thickness of the magnetite samples.

Molecular dynamics simulation (MDS) has been used in recent years as an effective approach for predicting thermophysical, rheological, and structural behavior of various materials [6-9]. In this method, atoms of a molecule are represented by many particles. The particles are initially located in a simulation box with a special arrangement and interact with each other by an appropriate potential function. Briefly, the MD method is based on deriving the equation of motion of every particle in the simulation box and integrating the differential equations to obtain the velocity and position of the particles [10]. These data are then used to calculate the main parameters of the simulation such as thermal conductivity.

MDS can be conducted in two ways in order to calculate the thermal conductivity, equilibrium molecular dynamic (EMD) and none equilibrium molecular dynamic (NEMD). In the EMD method, the system is equilibrated at a specific temperature and the thermal conductivity is calculated for the system at this stable condition. While, in the NEMD method, the simulation box is subjected to a prescribed temperature gradient. Thus, the heat flux through the system can be obtained from the temperature gradient and used for calculation of the thermal conductivity.

An extension of NEMD was proposed by Muller and Plathe [10]. This method applies NEMD in the reverse direction and is called reverse NEMD (rNEMD). That is, the imposed heat flux to a system results in a temperature gradient. In other words, the heat flux added to the system increases the kinetic energy. The kinetic energy is exchanged between the particles in the simulation box continuously. As a result, a temperature gradient is induced in the direction of the heat flux [12].

Chicot et al. [13] studied mechanical properties of magnetite utilizing MDS. Comparing the results with that of the experiments, they showed that MDS is an appropriate way to obtain Young's modulus, Poisson's ratio, and shear modulus. Moreover, the results obtained for pure oxides were shown to be very different from those determined for complex oxides. Hess et al. [14] performed an MDS in order to determine correlations in an aligned ferrofluid. They compared the

correlations with the results of an analytical approach.

Vaari [15] studied mass transport in bulk magnetite using MDS. In order to describe the interactions between atoms in the lattice, Buckingham potential in combination with the coulomb term was used. Results showed that the cause of ionic diffusion is vacancies in some cation and anion points in the lattice which is called Schottky defects. The diffusion coefficient was also calculated using the mean square displacement of magnetite atoms.

Regarding the reports mentioned above, a limited number of experimental data on the thermal conductivity of magnetite are available in the literature. There is also a lack of numerical studies on the thermal conductivity despite the growing application of the magnetic materials.

In the current research, MDS is carried out to calculate the thermal conductivity of magnetite. The effects of temperature and simulation box size on the thermal conductivity are also investigated.

Nomenclature

<i>MDS</i>	Molecular Dynamics Simulation
<i>EMD</i>	Equilibrium Molecular Dynamics
<i>NEMD</i>	None Equilibrium Molecular Dynamics
rNEMD	Reversed None Equilibrium Molecular Dynamics
<i>j</i>	Heat flux (W/m ²)
∇T	Temperature Gradient (K)
<i>r</i>	Distance between atoms (Å)
<i>N</i>	Number of slabs
<i>FCC</i>	Face centered cubic
<i>V</i>	Interatomic potential (kcal/mol)
<i>A</i>	Interatomic potential constant (kcal/mol)
<i>C</i>	Interatomic potential constant (kcalÅ ⁶ /mol)
<i>q</i>	Charge of the ions
<i>T</i>	Temperature (K)
<i>m</i>	Mass
<i>v</i>	Velocity
<i>k_b</i>	Boltzmann's constant
<i>t</i>	Time (second)
<i>L_x</i> and <i>L_y</i>	Cross-sectional lengths (m)
Greek	
κ	Thermal conductivity(W/m.K)

ρ Ionic-pair dependent length parameter (\AA)

Subscripts

i, j Ith and jth atom
 k Number of atoms
 h, c Hot and cold

2. Theory

Heat flux is proportional to the temperature gradient by the Fourier's law as given by

$$j = -\kappa \nabla T, \quad (1)$$

where κ is the thermal conductivity and is generally represented by a 3×3 tensor, however, the thermal conductivity of anisotropic material can be assumed to be a scalar with a specific value in all directions.

MDS can either obtain the temperature gradient of a bulk substance from induced heat flux to the system or vice versa. In the rNEMD method, heat flux is imposed on the system. Then, the temperature gradient of the whole system is deduced as a result of kinetic energy swapping between the layers. Thus, the thermal conductivity can be obtained from the known values of the temperature gradient and heat flux. This method is elaborated in Fig. 1.

As shown in Fig. 1, the simulation box is subdivided into N slabs where N is an even number. Due to the symmetry, the kinetic energy is swapped between slabs number 1

and $(N+1)/2$. Temperatures of the center and two ends of the simulation box will rise and decrease, respectively, after elapse of enough time,. Heat flux can be obtained from the kinetic energy of the system, and the average temperature gradient can then be calculated over time and all atoms in the simulation box [11].

3. Methodology

rNEMD Molecular Dynamics Method provided in the LAMMPS package is used for simulation of the thermal conductivity. The first issue in MDS is modeling the geometry and initial configuration of the simulation box. Magnetite (Fe_3O_4) has an inverse spinel structure of $(\text{Fe}^{2+})(\text{Fe}^{3+})_2\text{O}_4$ and an FCC crystal with unit cell edge length of $a=8.36\text{\AA}$. A normal spinel, such as FeCr_2O_4 , has the formula of AB_2O_4 with A atoms in the tetrahedral and B atoms in the octahedral sites. On the other hand, the inverse spinels have B atoms in the tetrahedral and both A and B atoms in the octahedral sites [16]. Thus, in magnetite crystal, Fe^{3+} cations fill the tetrahedral sites, and Fe^{2+} and the remaining Fe^{3+} cations randomly are distributed in the octahedral holes. The structure of the magnetite crystal is shown in Fig. 2.

The red, gray, blue, and yellow balls shown in Fig.2 are Fe^{3+} (tetrahedral sites), Fe^{3+} (octahedral sites), Fe^{2+} (octahedral sites), and oxygen ions, respectively.

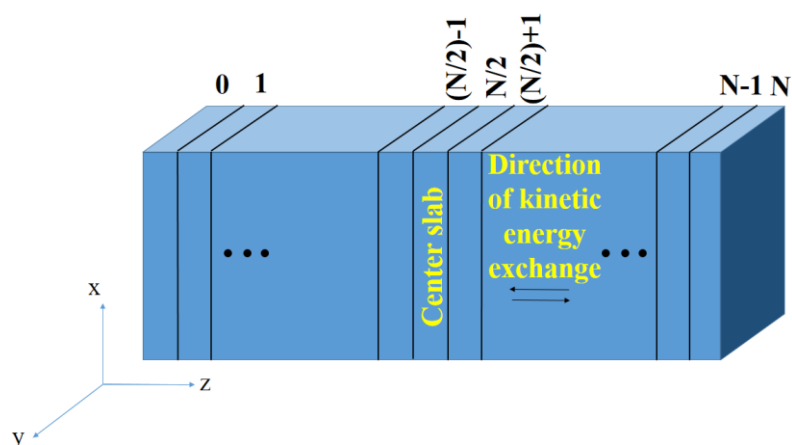


Fig. 1. Simulation box

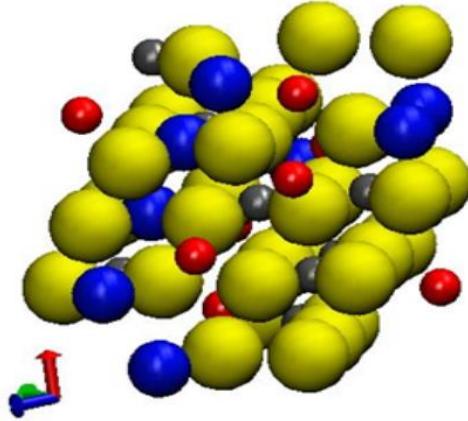


Fig.1. Crystal structure of magnetite

In order to simulate the interactions between ions, Buckingham potential in combination with Coulomb term, given by

$$V_{ij}(r_{ij}) = A_{ij} \exp\left(-\frac{r_{ij}}{\rho_{ij}}\right) - \frac{C_{ij}}{r_{ij}^6} + \frac{q_i q_j}{r_{ij}}, \quad (2)$$

is used, where r is the distance between the pair of atoms i and j . Moreover, A , C , and ρ are constants of the potential function, which are given in table 1.

The pair coefficients are extracted from various references [17], [18]. It is worth mentioning that the other pairs, such as cation-cation pairs (Fe^{3+} - Fe^{3+} , Fe^{2+} - Fe^{2+} , and Fe^{2+} - Fe^{3+}), are considered purely coulombic by setting the constants A and C to zero.

The periodic boundary condition is applied in all directions to avoid boundary effects. Moreover, the time step is set to 1 fs in all simulations.

Before running the main simulation, the system is subjected to the NVT ensemble for four ps. afterwards, in order to have a stable system, it is relaxed in the NVE ensemble and finally, the main simulations run up to 30 ps to reach the steady-state condition. The kinetic temperature of every slab can be calculated as.

$$T_k = \frac{\sum_{i \in k} m_i v_i^2}{3n_k k_b}, \quad (3)$$

where k denotes the number of atoms. m and v are mass and velocity of each particle, respectively and k_b is Boltzmann's constant. The temperature gradient along the simulation box can simply be calculated from the slabs temperatures. An energy balance implies that the sum of the kinetic energy of the system equals the total heat added to the system. Therefore, the thermal conductivity is calculated as

$$\kappa = -\frac{\sum \frac{m}{2} (v_h^2 - v_c^2)}{2tL_x L_y \langle \partial T / \partial z \rangle} \quad (4)$$

where L_x and L_y are the cross-sectional lengths of the simulation box and h and c indices denote hot and cold points, respectively.

4. Results and discussion

In order to validate the numerical method, thermal conductivity of solid argon is calculated at different temperatures and the MD results have been compared with data of ref. [19] and ref. [20], as shown in Fig. 3.

Table 1. Constants of Buckingham potential for magnetite

ions	A (kcal/mol)	ρ (Å)	C (kcalÅ ⁶ /mole)
$\text{Fe}^{2+} - \text{O}^{2-}$	16005.95	0.3399	0
$\text{Fe}^{3+} - \text{O}^{2-}$	32620.68	0.3128	0
$\text{O}^{2-} - \text{O}^{2-}$	220176.0	0.2192	737.92

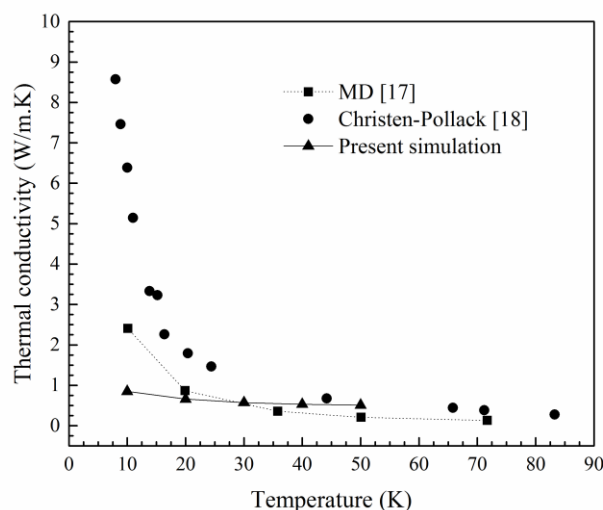


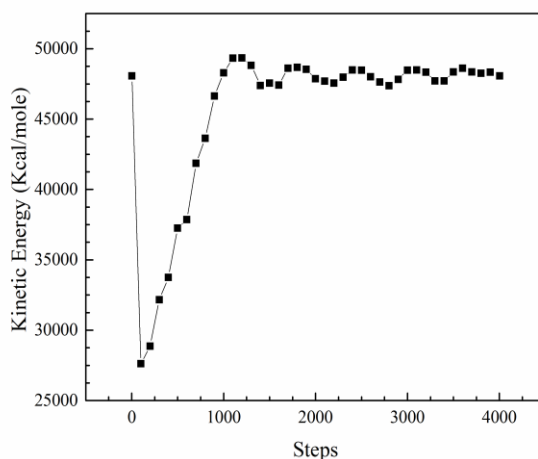
Fig. 2. Comparison between the results of present simulation and those of the refs [17] and [18] for thermal conductivity of solid argon

The thermal conductivity of solids at low temperatures is influenced by quantum effects. The criterion for considering these effects is Debye temperature [21]. Above Debye temperature, all vibrational modes are dominant and the quantum effect is negligible. Conversely, at temperatures below Debye temperature, the quantum effects become important and a quantum correction needs to be considered in order to calculate the thermal conductivity accurately. Debye temperature of solid argon is 92K. However, In MD simulations, quantum effects cannot be considered for temperatures below 161K [22]. As shown in Fig. 3, there is a good agreement between the current results, MD

results of ref. [19], and analytical results of ref. [20]. The deviation from the experimental results at temperatures below 20K is due to the quantum effects as described.

Simulations have been carried out at different box sizes and temperatures. Variation of the kinetic, potential, and total energy of the system with time at $T=400\text{K}$ are depicted in Fig.4 (a) to (c), respectively.

It can be observed in Fig. 4 that after relatively a long time, the kinetic, potential and total energies oscillate around a specific value. This convergence of the total energy of the system implies that the energy of the system is fully relaxed before the main simulation.



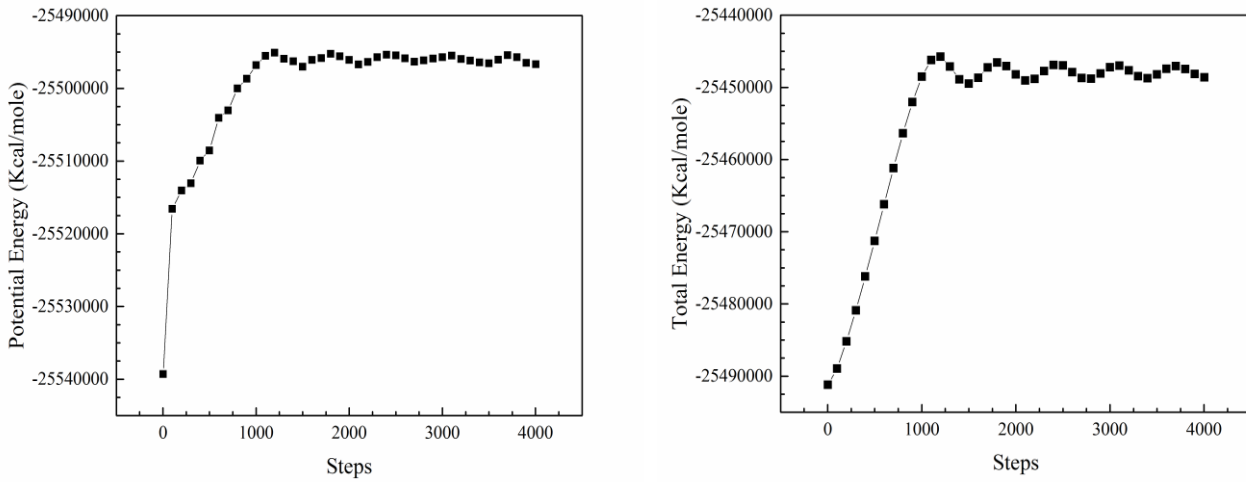


Fig.4. Kinetic, potential and total energy of magnetite crystal at 400K

Kinetic energy induced in the system which results from velocity exchange, is shown in Fig. 5 for different temperatures. The heat flux in the system is obtained by dividing this quantity by time and cross-sectional area.

According to Fig.5, the kinetic energy increases linearly with time. This behavior, as it shows, will be continued infinitely. Thus, the correct time to calculate the thermal conductivity is when the temperature distribution becomes linear across the simulation box. Figure 6 shows the variation

of temperature distribution in the simulation box with time.

As shown, approximately after 15000 time steps (15ns), the temperature gradient becomes linear.

The temperature distribution in the simulation box at different temperatures is depicted in Fig. 7.

The linearity of temperature distribution is essential in the Muller-Plathe method. As shown in Fig. 7. Although the temperature is almost linear, there are nonlinear parts at the beginning and middle of the simulation box.

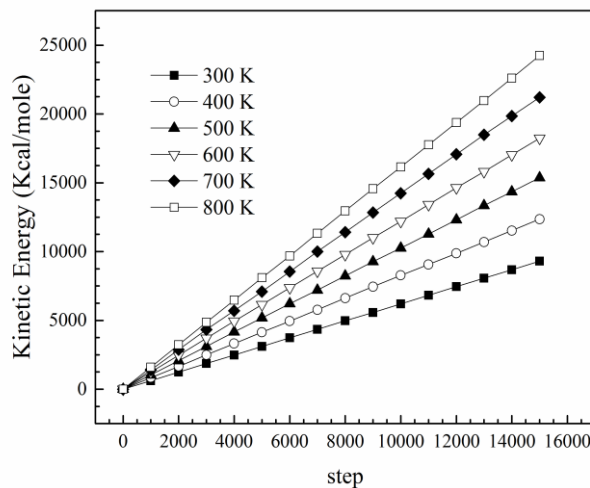


Fig.5. Kinetic energy variation at different simulation steps

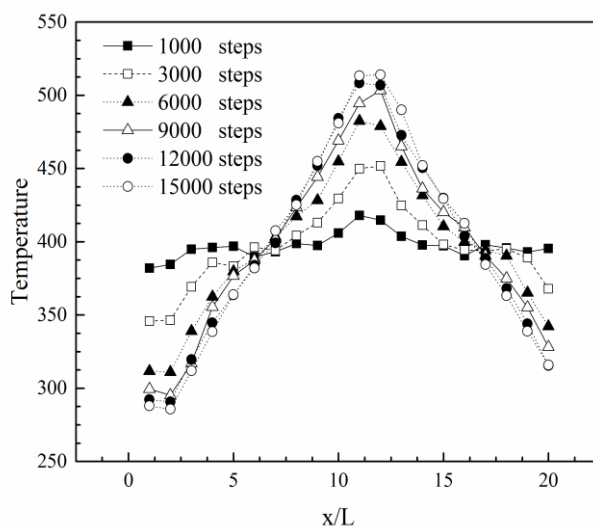


Fig.6. Temperature variation of the simulation box at 400K from 1000 to 15000 steps

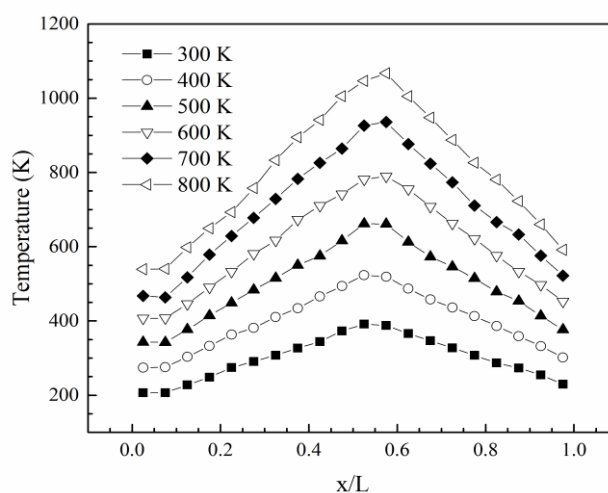


Fig.7. Temperature variation of the simulation box at different temperatures.

This nonlinearity at the edge of the simulation box is explained by phonon boundary scattering. This phenomenon causes a deviation of temperature from the linear shape in the boundary regions [24].

Data obtained from Figs. 5 and 7 are used in Eq. (4) for calculation of the thermal conductivity.

In order to check the size independency and ensure that the given box size is sufficient for reliable results, several primary simulations have been carried out with different grid sizes and the results have been represented in Fig. 8.

As shown in Fig. 8, the thermal conductivity increases by increasing the box size in the longitudinal direction, z . The thermal conductivity increase can be explained by the phonon mean free path [5]. As the box size increases and gets closer to the phonon mean free path, the number of phonons scattered from the boundaries decreases. In other words, as the simulation box size increases, more phonon mean free paths are considered [12], [21]. As a consequence, the results become more accurate in comparison with experimental data obtained for bulk systems.

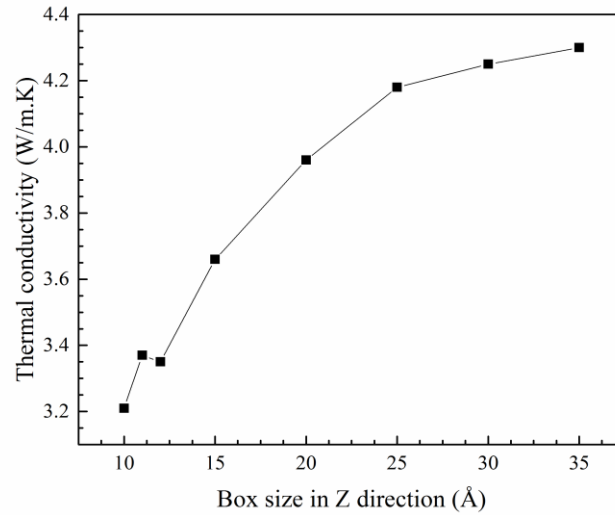


Fig.8. Effect of magnetite layer size on the thermal conductivity at 400K.

Figure 8 also indicates that the thermal conductivity varies slightly for box sizes greater than 20\AA in the z-direction. It should be noted that 20 multiplied by the unit cell constant equals 167.2\AA which is the actual grid size in the z direction.

Due to the computational costs, a $6\text{\AA} \times 6\text{\AA} \times 20\text{\AA}$ cubic unit cell has been considered for the rest of the simulations.

As mentioned before, there are non-linear parts in temperature distribution in the

simulation box due to the phonon-boundary scattering. This non-linearity is a source of error and affects the accuracy of the results. In order to overcome this problem, another set of simulations has been carried out considering only the part of the simulation box where the temperature is linear, $(0.125L < x < 0.475)$ [10]. Variation of the magnetite thermal conductivity with temperature obtained from both numerical approaches along with experimental results of ref. [7] are shown in Fig. 9.

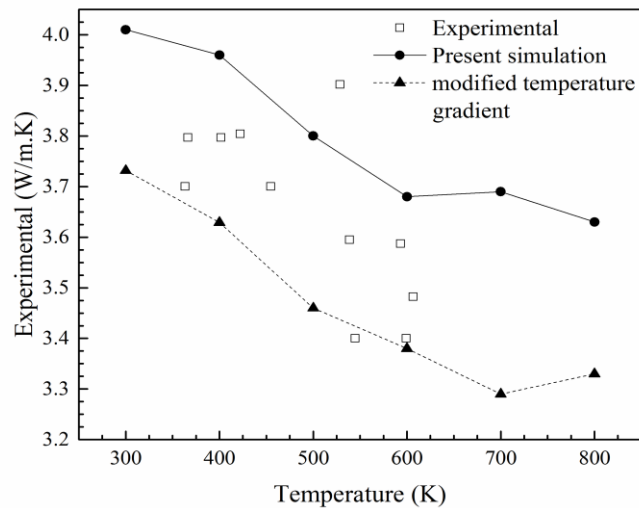


Fig.9. Thermal conductivity of bulk magnetite at the temperature range of 300K- 800K.

Figure 9 shows a good agreement between numerical and experimental results especially at intermediate temperatures. The results obtained from the modified method are shown to be closer to the experimental data. The decreasing trend of thermal conductivity is also predicted by the numerical simulation. Two mechanisms named phonon boundary and phonon-phonon Um Klapp scattering are responsible for decreasing thermal conductivity with temperature. Moreover, Results indicate that Buckingham potential function is an appropriate potential to evaluate the thermal properties of magnetite.

5. Conclusions

Molecular dynamic simulation has been carried out to calculate the thermal conductivity of magnetite. The effects of temperature and magnetite layer size on the thermal conductivity have been investigated. A comparison of the results with the available experimental data indicates that the thermal conductivity of magnetite can be predicted appropriately using Buckingham potential function. Results also show that the thermal conductivity of magnetite decreases with an increase in the temperature.

References

- [1] Masaaki Motozawa, Jia Chang, Tatsou Sawada, Yasuo Kawaguchi, "Effect of Magnetite Field on Heat Transfer in Rectangular Duct Flow of a Magnetite Fluid," 12th International Conference on Magnetic Fluids, Physics Procedia 9 (2010) 190-193.
- [2] Mohammad Hassan Omid, Mahboobeh Alibeygi, Farideh Piri, Mohammad Masoudifard, "Polystyrene/magnetite nanocomposite synthesis and characterization: investigation of magnetite and electrical properties for using as microelectromechanical systems (MEMS)," Materials Science-Poland, 35(1), 2017, pp, 105-110
- [3] J. Molgaard and W. W. Smeltzer, "Thermal conductivity of magnetite and hematite," J. Appl. Phys., vol. 42, no. 9, pp. 3644–3647, 1971.
- [4] SYDNEY P. Clark, "Handbook of physical constants," The Geological Society of America Memoir, PP. 461-482, 1996.
- [5] N.-W. Park et al., "Reduced temperature-dependent thermal conductivity of magnetite thin films by controlling film thickness.," Nanoscale Res. Lett., vol. 9, no. 1, p. 96(8pp), 2014.
- [6] H. Aminfar, N. Razmara, and M. Mohammadpourfard, "Molecular dynamics study of ferrofluid flow inside nanochannels under magnetic fields," J. Comput. Theor. Nanosci., vol. 12, no. 9, pp. 2339–2347, Sep. 2015.
- [7] A. R. bin Saleman, H. K. Chilukoti, G. Kikugawa, M. Shibahara, and T. Ohara, "A molecular dynamics study on the thermal transport properties and the structure of the solid-liquid interfaces between face-centered cubic (FCC) crystal planes of gold in contact with linear alkane liquids," Int. J. Heat Mass Transf., vol. 105, pp. 168–179, Feb. 2017.
- [8] A. Vegiri and E. I. Kamitsos, "Molecular dynamics study of structural reorganization by electro-thermal poling in sodium diborate glass," J. Non. Cryst. Solids, vol. 472, pp. 14–24, Sep. 2017.
- [9] L. Momenzadeh, B. Moghtaderi, O. Buzzi, X. Liu, S. W. Sloan, and G. E. Murch, "The thermal conductivity decomposition of calcite calculated by molecular dynamics simulation," Comput. Mater. Sci., vol. 141, pp. 170–179, 2018.
- [10] M. E. Tuckerman, "Statistical Mechanics: Theory and Molecular Simulation," p. 720, 2010.
- [11] F. Müller-Plathe, "A simple nonequilibrium molecular dynamics method for calculating the thermal conductivity," J. Chem. Phys., vol. 106, no. 14, pp. 6082–6085, 1997.
- [12] J. Severin and P. Jund, "Thermal conductivity calculation in anisotropic crystals by molecular dynamics: Application to α -Fe₂O₃," J. Chem. Phys., vol. 146, no. 5, 2017.

- [13] D. Chicot et al., "Mechanical properties of magnetite (Fe_3O_4), hematite ($\alpha\text{-Fe}_2\text{O}_3$) and goethite ($\alpha\text{-FeO}\cdot\text{OH}$) by instrumented indentation and molecular dynamics analysis," *Mater. Chem. Phys.*, vol. 129, no. 3, pp. 862–870, 2011.
- [14] S. Hess, J. B. Hayter, and R. Pynn, "A comparison of molecular dynamics and analytic calculation of correlations in an aligned ferrofluid," *Mol. Phys.*, vol. 53, no. 6, pp. 1527–1533, 1984.
- [15] J. Vaari, "Molecular dynamics simulations of vacancy diffusion in chromium(III) oxide, hematite, magnetite and chromite," *Solid State Ionics*, vol. 270, pp. 10–17, 2015.
- [16] R. M. Cornell and U. Schwertmann, *Iron Oxides*. ISBN: 3-527-30274-3 . 2003.
- [17] L. Minervini, M. O. Zacate, and R. W. Grimes, "Defect cluster formation in M_2O_3 -doped CeO_2 ," *Solid State Ionics*, vol. 116, no. 3, pp. 339–349, Jan. 1999.
- [18] G. V Lewis and C. R. A. Catlow, "Potential models for ionic oxides," *J. Phys. C Solid State Phys.*, vol. 18, no. 6, pp. 1149–1161, Feb. 1985.
- [19] S. Y. Hideo Kaburaki, Ju Li, "Thermal Conductivity of Solid Argon by Classical Molecular Dynamics," *Mat. Res. Soc. Symp. Proc. Mater. Res. Soc.*, vol. 538, no. 0, pp. 503–508, 1999.
- [20] D. K. Christen and G. L. Pollack, "Thermal conductivity of solid argon," *Phys. Rev. B*, vol. 12, no. 8, pp. 3380–3391, 1975.
- [21] M. Alaghemandi, E. Algaer, M. C. Böhm, and F. Müller-Plathe, "The thermal conductivity and thermal rectification of carbon nanotubes studied using reverse non-equilibrium molecular dynamics simulations," *Nanotechnology*, vol. 20, no. 11, 2009.
- [22] A. Soleimani, H. Araghi, Z. Zabihi, and A. Alibakhshi, "A comparative study of molecular dynamics simulation methods for evaluation of the thermal conductivity and phonon transport in Si nanowires," *Comput. Mater. Sci.*, vol. 142, pp. 346–354, 2018.
- [23] J. R. Lukes and H. Zhong, "Thermal Conductivity of Individual Single-Wall Carbon Nanotubes," *J. Heat Transfer*, vol. 129, no. 6, p. 705, 2007.
- [24] M. Khalkhali and F. Khoeini, "Impact of torsion and disorder on the thermal conductivity of Si nanowires: A nonequilibrium molecular dynamics study," *J. Phys. Chem. Solids*, vol. 112, pp. 216–221, 2018.